GLOBAL CLIMATE

An astronomically dated record of Earth's climate and its predictability over the last 66 million years

Thomas Westerhold[1]*, Norbert Marwan[2,3], Anna Joy Drury[1,4], Diederik Liebrand[1], Claudia Agnini[5], Eleni Anagnostou[6], James S. K. Barnet[7,8], Steven M. Bohaty[9], David De Vleeschouwer[1], Fabio Florindo[10,11], Thomas Frederichs[1,12], David A. Hodell[13], Ann E. Holbourn[14], Dick Kroon[15], Vittoria Lauretano[16], Kate Littler[7], Lucas J. Lourens[17], Mitchell Lyle[18], Heiko Pälike[1], Ursula Röhl[1], Jun Tian[19], Roy H. Wilkens[20], Paul A. Wilson[9], James C. Zachos[21]

Much of our understanding of Earth's past climate comes from the measurement of oxygen and carbon isotope variations in deep-sea benthic foraminifera. Yet, long intervals in existing records lack the temporal resolution and age control needed to thoroughly categorize climate states of the Cenozoic era and to study their dynamics. Here, we present a new, highly resolved, astronomically dated, continuous composite of benthic foraminifer isotope records developed in our laboratories. Four climate states—Hothouse, Warmhouse, Coolhouse, Icehouse—are identified on the basis of their distinctive response to astronomical forcing depending on greenhouse gas concentrations and polar ice sheet volume. Statistical analysis of the nonlinear behavior encoded in our record reveals the key role that polar ice volume plays in the predictability of Cenozoic climate dynamics.

G lobal changes in Earth's climate during the Cenozoic era, the last 66 million years, have long been inferred from stable-isotope data in carbonate shells of benthic foraminifera, which are single-celled amoeboid organisms that live on the seafloor. Stable carbon and oxygen isotope records from deep-sea benthic foraminifera are a proven, invaluable archive of long-term changes in Earth's carbon cycle, deep-sea temperature, and seawater composition driven by changes in ice volume (1, 2). In 1975, Shackleton and Kennett (3) produced one of the first deep-sea benthic foraminifer stable isotope records of the Cenozoic. Despite being of low temporal resolution, it revealed that Earth's climate had transitioned from a warm state 60 to 40 million years ago (Ma) to a cool state 10 to 5 Ma. Over the last 45 years, many deep-sea benthic foraminifer stable-isotope records of variable length and quality have been developed, resulting in a more detailed record of Cenozoic climate change. Compilations of these deep-sea isotope records provide a compelling chronicle of past trends, cyclic variations, and transient events in the climate system from the Late Cretaceous to today (1, 4–10). However, even the most recent benthic isotope compilations cannot accurately document the full range and detailed characteristics of Cenozoic climate variability on

time scales of 10 thousand to 1 million years. Age models and temporal resolution of Cenozoic benthic isotope compilations are too coarse and/or include gaps, particularly before 34 Ma. These weaknesses hamper progress in determining the dynamics of the Cenozoic climate system (4, 9, 11), for example, because they prohibit application of advanced techniques of nonlinear time series analysis at the required (astronomical) time scales. The lack of highly resolved, continuous, and accurately dated records constitutes a key limitation in our ability to identify and understand the characteristics of Earth's evolving climate during the Cenozoic.

Here, we present a new astronomically tuned deep-sea benthic foraminifer carbon ($\delta^{13}C$) and oxygen ($\delta^{18}O$) isotope reference record uniformly covering the entire Cenozoic, developed in our laboratories by using sediment archives retrieved by the International Ocean Discovery Program and its predecessor programs (Fig. 1). To produce this composite record, we selected 14 ocean drilling records, checked and revised their composite splices if necessary, and preferentially selected records using the genera *Cibicidoides* and *Nuttallides* to minimize systematic interspecies isotopic offsets (1, 4, 12, 13). We additionally generated new benthic stable-isotope data spanning the late Miocene and

middle to late Eocene to fill intervals inadequately covered by existing records. We collated existing astrochronologies for all records, recalibrated them to the La2010b orbital solution (14) if required, and developed an astrochronology for the middle to late Eocene (13). We estimate our chronology to be accurate to ±100 thousand years (kyr) for the Paleocene and Eocene, ±50 kyr for the Oligocene to middle Miocene, and ±10 kyr for the late Miocene to Pleistocene. The composite record is affected by some spatial biases arising from the uneven distribution of deep-sea stable isotope data that mainly derive from low to mid-latitudes (13). Nevertheless, the resulting Cenozoic Global Reference benthic foraminifer carbon and oxygen Isotope Dataset (CENOGRID) provides a refined record with higher signal-to-noise ratio than any previous compilations (13) (supplementary text S1) and better coverage of the Paleocene, Eocene, and late Miocene intervals (fig. S32). The CENOGRID serves as an astronomically tuned, high-definition stratigraphic reference of global climate evolution for the past 66 million years.

On time scales of 10 thousand to 1 million years, global climate is a complex, dynamical system responding nonlinearly to quasi-periodic astronomical forcing. By combining the latest high-resolution generation of Cenozoic deep-sea isotope records on a highly accurate time scale, CENOGRID enables the definition of Earth's fundamental climates and investigation of the predictability of their dynamics. We used recurrence analysis (RA) of the CENOGRID record (13, 15) to identify fundamental climate states that internally share characteristic and statistically distinctive dynamics. Recurrence is a major property of dynamical systems, and RA provides information about nonlinear dynamics, dynamical transitions, and even nonlinear interrelationships (15) and facilitates evaluation of underlying dynamical processes—e.g., whether they are stochastic, regular, or chaotic. We present recurrence plots and their quantification of the benthic foraminifer $\delta^{13}C$ and $\delta^{18}O$ records to recognize different climate states and apply the RA measure of "determinism" (DET) to quantify the predictability of Cenozoic climate dynamics.

Four distinctive climate states emerge as separate blocks from our recurrence plots of the $\delta^{18}O$ CENOGRID record, which we designate as

[1]MARUM–Center for Marine Environmental Sciences, University of Bremen, 28359 Bremen, Germany. [2]Potsdam Institute for Climate Impact Research (PIK), Member of the Leibniz Association, 14412 Potsdam, Germany. [3]University of Potsdam, Institute of Geosciences, 14469 Potsdam, Germany. [4]Department of Earth Sciences, University College London, Gower Street, London WC1E 6BT, UK. [5]Dipartimento di Geoscienze, Università degli Studi di Padova, Via Gradenigo 6, I-35131 Padova, Italy. [6]GEOMAR Helmholtz-Zentrum für Ozeanforschung Kiel, Wischhofstrasse 1-3, 24148 Kiel, Germany. [7]Camborne School of Mines and Environment and Sustainability Institute, University of Exeter, Penryn Campus, Penryn, UK. [8]School of Earth and Environmental Sciences, University of St Andrews, St Andrews, Scotland, UK. [9]Ocean and Earth Science, University of Southampton, National Oceanography Centre, Southampton, UK. [10]Istituto Nazionale di Geofisica e Vulcanologia, INGV, Rome, Italy. [11]Institute for Climate Change Solutions, Pesaro e Urbino, Italy. [12]Faculty of Geosciences, University of Bremen, Bremen, Germany. [13]Godwin Laboratory for Palaeoclimate Research, Department of Earth Sciences, University of Cambridge, Cambridge, UK. [14]Institute of Geosciences, Christian-Albrechts-University, Kiel 24118, Germany. [15]School of GeoSciences, University of Edinburgh, Edinburgh, UK. [16]School of Chemistry, University of Bristol, Bristol BS8 1TS, UK. [17]Department of Earth Sciences, Faculty of Geosciences, Utrecht University, Princetonlaan 8a, 3584 CB Utrecht, Netherlands. [18]College of Earth, Ocean, and Atmospheric Science, Oregon State University, Corvallis, OR 97331, USA. [19]State Key Laboratory of Marine Geology, Tongji University, Siping Road 1239, Shanghai 200092, PR China. [20]School of Ocean and Earth Science and Technology, University of Hawaii, Honolulu, HI 96822, USA. [21]Department of Earth and Planetary Sciences, University of California, Santa Cruz, California, USA.
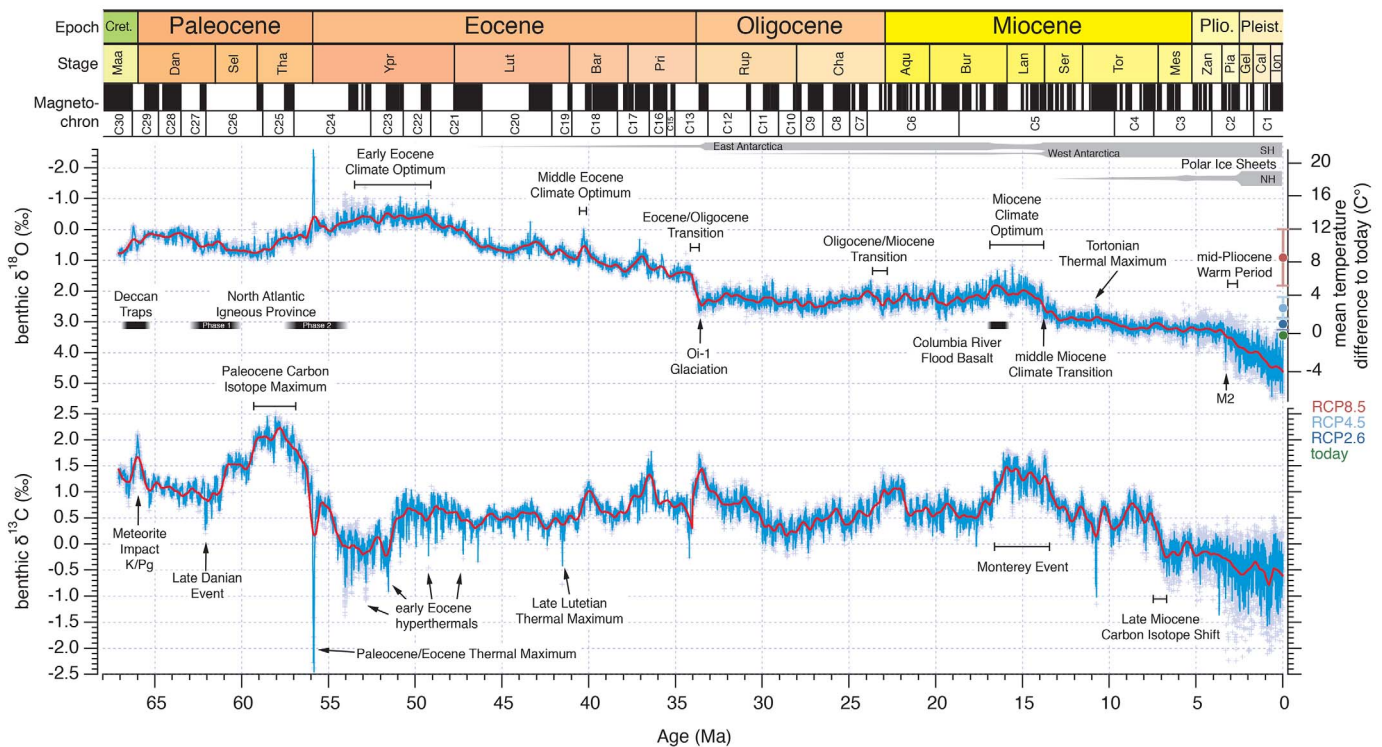*Corresponding author. Email: twesterhold@marum.de

Fig. 1. Cenozoic Global Reference benthic foraminifer carbon and oxygen Isotope Dataset (CENOGRID) from ocean drilling core sites spanning the past 66 million years. Data are mostly generated by using benthic foraminifera tests of the taxa *Cibicidoides* and *Nuttallides* extracted from carbonate-rich deep-sea sediments drilled during Ocean Drilling Program (ODP) and Integrated Ocean Drilling Program (IODP) expeditions. Genus-specific corrections were applied and oxygen isotope data adjusted by +0.64‰ and +0.4‰, respectively (*12*), with the green dot indicating the average oxygen isotope composition of the last 10 kyr. Average resolution for the interval from 0 to 34 Ma is one sample every 2 ky; for the interval from 34 to 67 Ma, it is one sample every 4.4 kyr. After binning, data were resampled and smoothed by a locally weighted function over 20 kyr (blue curve) and 1 Myr (red curve) to accentuate the different rhythms and trends in Earth's carbon cycle and temperature operating on various time scales. Oxygen isotope data have been converted to average temperature differences with respect to today (*13*). Future projections for global temperature (*44*) in the year 2300 are shown by plotting three representative concentration pathways (RCP) scenarios (light blue, dark blue, and red dots). Gray horizontal bars mark rough estimates of ice volume in each hemisphere. Absolute ages for epochs and stages of the Cenozoic (GTS2012) and geomagnetic field reversals (this study) are provided for reference. The oxygen isotope data axis is reversed to reflect warmer temperatures at times of lower $\delta^{18}O$ values. Aqu, Aquitanian; Bur, Burdigalian; Cal, Calabrian; Cha, Chattian; Cret., Cretaceous; Dan, Danian; Gel, Gelasian; Ion, Ionian; K/Pg, Cretaceous/Paleogene boundary; Lan, Langhian; Lut, Lutetian; M2, first major glacial event in the NH; Maa, Maastrichtian; Mes, Messinian; NH, Northern Hemisphere; Oi-1, the first major glacial period in the Oligocene; Pia, Piacenzian; Pleist., Pleistocene; Plio., Pliocene; Pri, Priabonian; Rup, Rupelian; Sel, Selandian; Ser, Serravallian; SH, Southern Hemisphere; Tha, Thanetian; Tor, Tortonian; Ypr, Ypresian; Zan, Zanclean.

the Hothouse, Warmhouse, Coolhouse, and Icehouse states (Fig. 2). Blocklike structures in the recurrence plots identify epochs where the dynamical system is "trapped" in a particular state. This interpretation of Cenozoic climate history is broadly consistent with previous interpretations, but our recurrence plot analysis of the highly resolved CENOGRID data provides a more statistically robust and objective exposition of events.

Characteristic features of the four climate states can be inferred from the isotope profiles (Fig. 1) and scatterplots of the CENOGRID $\delta^{13}C$ and $\delta^{18}O$ data and from atmospheric CO_2 concentration estimates (Fig. 2) (*13*). Warmhouse and Hothouse states prevailed from the Cretaceous/Paleogene boundary (K/Pg, 66 Ma) to the Eocene-Oligocene Transition (EOT, 34 Ma). During the Warmhouse, global temperatures were more than 5°C warmer than they are today (*13*), and benthic $\delta^{13}C$

and $\delta^{18}O$ show a persistent positive correlation with one another. The Hothouse operated between the Paleocene-Eocene Thermal Maximum at 56 Ma and the end of the Early Eocene Climate Optimum (EECO) at 47 Ma (*16*), when temperatures were more than 10°C warmer than they are today and displayed greater amplitude variability. Transient warming events (hyperthermals) are an intrinsic feature of the Hothouse, wherein paired negative excursions in $\delta^{13}C$ and $\delta^{18}O$ reflect warming globally through rapid addition of carbon to the ocean-atmosphere system. The two Warmhouse phases from 66 to 56 Ma (Paleocene) and 47 to 34 Ma (middle-late Eocene) share a similar temperature range but have distinct background $\delta^{13}C$ isotope values and atmospheric CO_2 concentrations (Fig. 2 and fig. S35). At the EOT, the Warmhouse transitioned into the Coolhouse state, marked by a stepwise, massive drop in temperature and a

major increase in continental ice volume with large ice sheets appearing on Antarctica (*17*) to establish a unipolar glacial state (*18*). The recurrence plots mark out the EOT as the most prominent transition of the whole Cenozoic, which highlights the important role of ice sheets in modulating Earth's climate state (fig. S33) (*13*).

The Coolhouse state spans ~34 Ma (EOT) to 3.3 Ma (mid-Pliocene M2 glacial) and is divided into two phases by the marked shift in $\delta^{18}O$ increase at 13.9 Ma related to the expansion of Antarctic ice sheets during the middle Miocene Climate Transition (mMCT) (*19*). Warmer conditions culminating in the Miocene Climatic Optimum (MCO; ~17 to 14 Ma) (*20*) characterize the first phase, followed by cooling and increasing $\delta^{18}O$ during the second phase (Fig. 2). RA of carbon isotope data documents an additional major transition in the carbon cycle around 7 Ma related to the
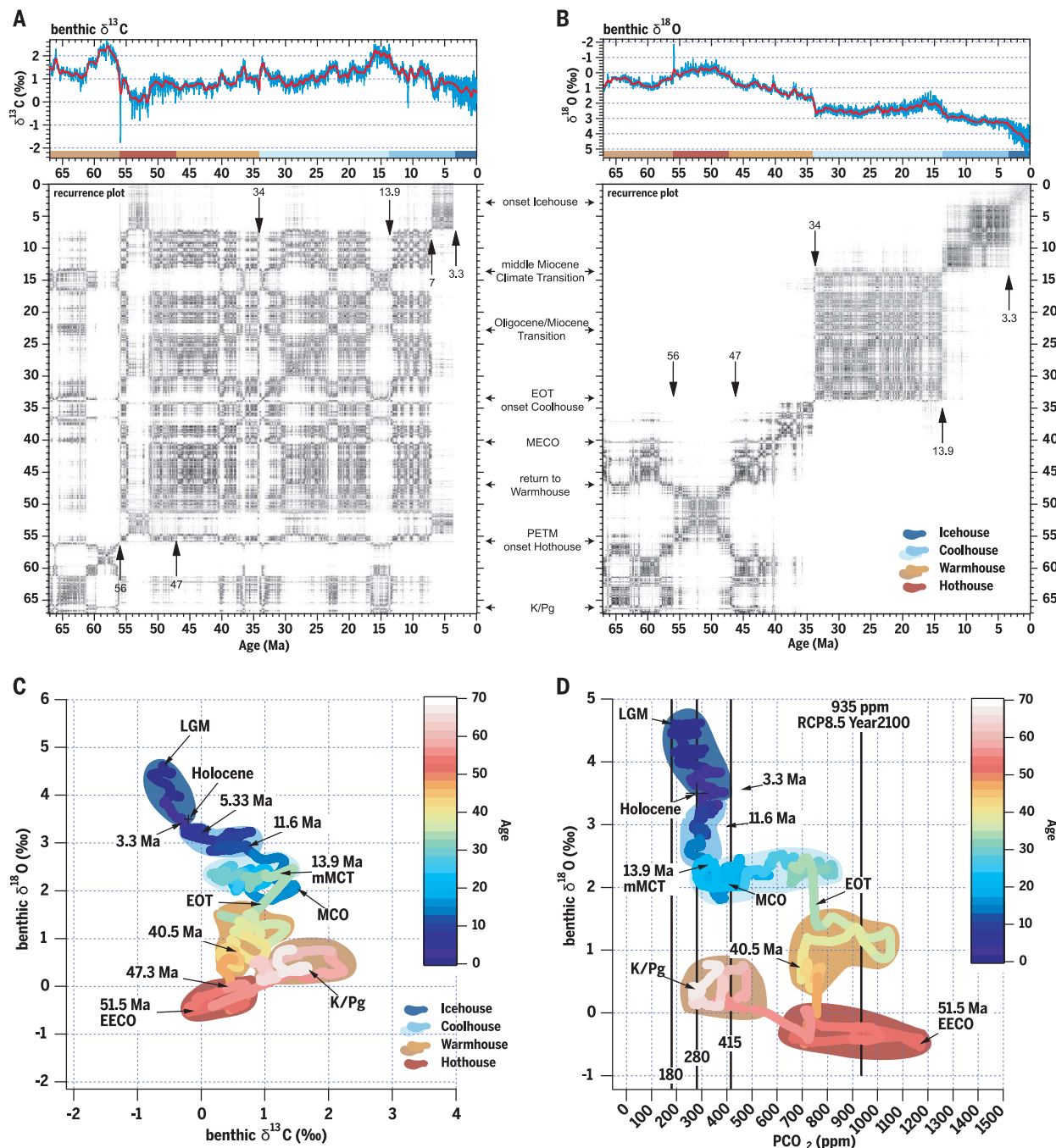
Fig. 2. Climate states of the Cenozoic. Deep-sea benthic foraminifer high-resolution carbon (**A**) and oxygen (**B**) isotope records and the respective recurrence plots as well as scatterplots of long-term benthic foraminifer carbon versus oxygen values (**C**) and oxygen values versus atmospheric CO_2 concentrations (**D**). Recurrence analysis compares climate change patterns occurring in a specific interval to the entire record. If climate dynamics have similar patterns, they will show up as darker areas in the plot; if they have no common dynamics, the plot will remain white. Four distinct climate states can be identified as Hothouse, Warmhouse, Coolhouse, and Icehouse with distinct transitions among them. The relation of oxygen isotopes, representative for average global temperature trends, to atmospheric CO_2 concentrations suggests that the present climate system as of today [415 parts per million (ppm) CO_2] is comparable to the Miocene Coolhouse close to the MCO. If CO_2 emissions continue unmitigated until 2100, as assumed for the RCP8.5 scenario, Earth's climate system will be moved abruptly from the Icehouse into the Warmhouse or even Hothouse climate state. LGM, Last Glacial Maximum; MECO, Middle Eocene Climate Optimum; PETM, Paleocene/Eocene Thermal Maximum.

end of the late Miocene carbon isotope shift (*11, 21, 22*). A major change in the correlation between benthic foraminifer $\delta^{13}C$ and $\delta^{18}O$ occurs during the Pliocene epoch (*23*). The Icehouse climate state (Fig. 2), driven by the appearance of waxing and waning ice sheets in the Northern Hemisphere, was fully established by the Pliocene-Pleistocene transition (*24*) (Figs. 1 and 2) with Marine Isotope Stage M2 at 3.3 Ma being a possible harbinger. The recurrence plots are less pronounced and more transparent from 3.3 Ma to today (Fig. 2 and fig. S34), suggesting that Earth's climate cryosphere dynamics entered a state not comparable to anything seen in the preceding 60 or more million years.
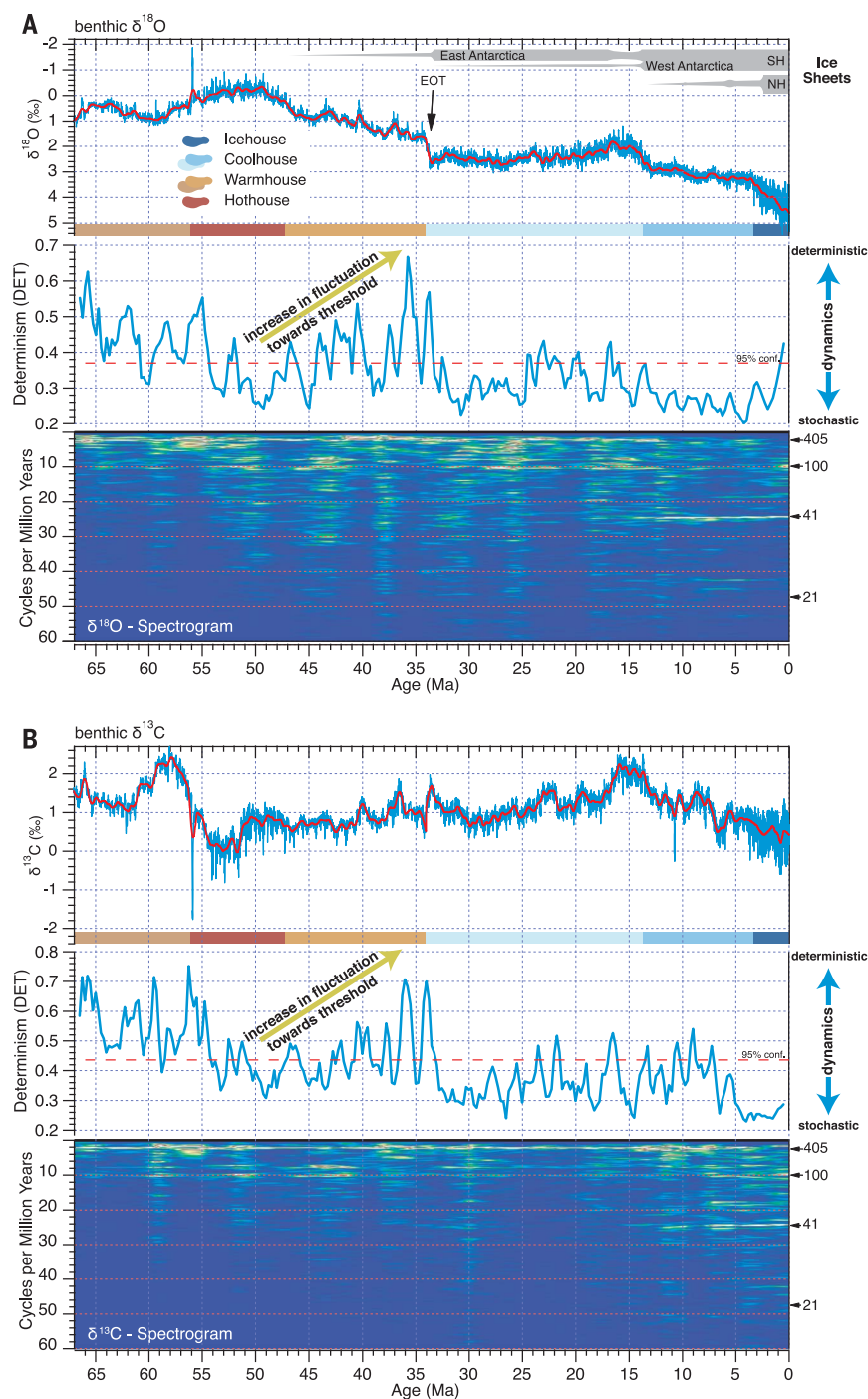
Fig. 3. Quasi-periodic changes and determinism in the global reference carbon cycle and oxygen isotope record. Evolutionary fast Fourier transform (FFT) spectrogram, recurrence determinism analysis, and benthic foraminifer oxygen (**A**) and carbon (**B**) isotope data plotted on age with the four climate states. Frequencies between 2 and 60 cycles per million years are related to changes in Earth's orbital parameters, known as Milankovitch cycles. The FFT spectrograms were computed with a 5-Myr window on the detrended records of benthic carbon and oxygen isotope data. From 67 to 13.9 Ma, cyclic variations in global climate are dominated by the eccentricity cycles of 405 and 100 kyr. Thereafter, in particular in the oxygen isotope record, the influence of obliquity increased, dominating the rhythm of climate in the record younger than ~7.7 Ma. Recurrence analysis of determinism (DET) shows that climate in the Warmhouse state is more deterministic (predictable) than in the Hothouse, Coolhouse, and Icehouse. From 47 Ma toward the EOT at 34 Ma, climate dynamic changes are rising in amplitude, approaching a threshold in the climate system. If DET tends to low values, the dynamics are stochastic, whereas high values represent deterministic dynamics.

The CENOGRID allows us to scrutinize the state dependency of climate system response to CO_2 and astronomical forcing on time scales of 10 thousand to 1 million years (13). Astronomical forcing throughout the Cenozoic is consistently uniform, but the RA indicates that the nonlinear response in climate variability to this forcing is strongly influenced by the fundamental state of climate. Evolutionary spectrograms characterize the dominant climatic response to astronomical forcing during the Cenozoic (Fig. 3). We find that the prevailing climate state, as characterized by atmospheric CO_2 concentration and polar ice sheets, orchestrates the response of climate processes to astronomical forcing. Modeled insolation-driven global temperature variability on astronomical time scales suggests that different temperature-response regimes exist: Eccentricity dominates temperature responses in low latitudes, precession in mid-latitudes, and obliquity in high latitudes (25). Thus, pronounced astronomical cyclicity in the CENOGRID could reflect climate state–dependent amplifications of latitude-specific climate processes.

In the Hothouse and Warmhouse, as well as the first Coolhouse phase, eccentricity-related cycles dominate the CENOGRID records, indicating a strong influence of low-latitude processes on climate variations. Obliquity-related cycles are sparse in these intervals but have been documented in other geochemical records (26, 27), exhibiting perhaps local lithological responses. Weak response in the obliquity band during the Hothouse and Warmhouse intervals might be related to the absence of a high-latitude ice sheet that could have amplified climate response to obliquity forcing. The driving mechanism for the prevailing eccentricity cyclicity in the benthic $\delta^{13}C$ and $\delta^{18}O$ records is still unknown, but modeling suggests that low- and mid-latitude processes in the climate system respond in a nonlinear way to insolation forcing (25, 28–30). In this regard, a key feedback likely involves the hydrological cycle with highly seasonal precipitation patterns during intervals of strong monsoon response to precession-induced insolation change, which could play a major role in the global distribution of moisture and energy (31–34). The expression of precession is apparently weak in the CENOGRID composite record, despite the dominant eccentricity forcing, likely owing to the long residence time of carbon in the oceans enhancing longer forcing periods (30, 35), as well as our strategy to avoid "overtuning" the record. After the increasing influence of high-latitude cooling and ice growth during the second Coolhouse phase, the obliquity-band response steadily increases after the mMCT before dominating climate dynamics by the late Miocene–early Pliocene (11, 22, 36). In the Icehouse state, the progressive decrease in

atmospheric CO_2 and major growth of polar ice sheets, which enhanced variability in $\delta^{18}O$, steadily amplified the influence of complex high-latitude feedbacks until they essentially dominated climate dynamics.

To better understand the complexity of climate dynamics recorded in the CENOGRID, we computed the RA measure of DET (13). This parameter quantifies the predictability of dynamics in a system's state. Predictability estimates the stochastic (unpredictable) versus the deterministic (predictable) nature of climate dynamics recorded in CENOGRID (13). DET values near zero correspond to unpredictable dynamics, whereas large values indicate predictable dynamics, which are especially interesting to examine on the approach to tipping points. Changes in DET can thus reveal transitions between fundamentally different climate regimes.

Our RA suggests that climate dynamics during the Warmhouse and Hothouse Cenozoic states are more predictable or more regular than those of the Coolhouse and Icehouse states (Fig. 3). The growth of polar ice sheets at the EOT enhanced the effect of obliquity pacing of high-latitude climate that interacted with eccentricity-modulated precession forcing at lower latitudes from that point in time. This led to increased nonlinear interactions among astronomically paced climate processes and, thus, more complex, stochastic climate dynamics. The development of a large Antarctic ice volume at the inception of the Coolhouse is associated with a fundamental regime change toward less predictable climate variability (lower DET values calculated from benthic $\delta^{18}O$) (Fig. 3). From 25 to 13.9 Ma DET is elevated again, related to a reduction in ice volume in relatively warmer times of the Coolhouse, culminating in the MCO. Despite the growing influence of ice sheets in the Coolhouse, until ~6 to 7 Ma, carbon-cycle dynamics remain more deterministic than temperature because $\delta^{13}C$ variations are predominantly driven by low-latitude processes and less strongly influenced by the complex interaction with polar ice-sheet fluctuations. After ~6 Ma DET drops, likely because of a stronger cryosphere imprint on the carbon cycle. Upon initiation of the Icehouse at 3.3 Ma, $\delta^{18}O$ recorded climate dynamics become slightly more deterministic (37) and carbon-cycle dynamics unpredictable, likely resulting from the complex response to the waxing and waning of polar ice caps (38).

The CENOGRID spectrogram displays a broader frequency range during several intervals with low DET values (e.g., Coolhouse), whereas high DET values (e.g., Warmhouse) occur when single frequencies dominate (Fig. 3). This could be signaling a more direct response to astronomical forcing in the Warmhouse compared with that in the Coolhouse. Our RA suggests

that the Hothouse is more stochastic (less predictable) than the Warmhouse, presumably induced by the occurrence of extreme hyperthermal events and their strong nonlinear and much-amplified climate response to astronomical forcing (39, 40). The evolving pattern in the DET from the onset of cooling after the EECO to the EOT is pronounced (Fig. 3). The amplitude in fluctuations between stochastic and deterministic dynamics intensifies from 49 Ma to 34 Ma, consistent with how Earth's climate system is suggested to behave (41, 42) as it moves toward a major tipping point. Once that tipping point is reached at the EOT, a rapid shift toward more permanently stochastic dynamics marks the inception of a new climate state (43). Thus, not only is polar ice volume critical to defining Earth's fundamental climate state, it also seems to play a crucial role in determining the predictability of its climatological response to astronomical forcing.

REFERENCES AND NOTES

1. J. Zachos, M. Pagani, L. Sloan, E. Thomas, K. Billups, *Science* **292**, 686–693 (2001).
2. K. G. Miller, G. Mountain, J. D. Wright, J. V. Browning, *Oceanography (Wash. D.C.)* **24**, 40–53 (2011).
3. N. J. Shackleton, J. P. Kennett, in *Initial Reports of the Deep Sea Drilling Project* (U.S. Government Printing Office, 1975), vol. 29, pp. 743–755.
4. B. S. Cramer, J. R. Toggweiler, J. D. Wright, M. E. Katz, K. G. Miller, Ocean overturning since the Late Cretaceous: Inferences from a new benthic foraminiferal isotope compilation. *Paleoceanography* **24**, PA4216 (2009).
5. D. De Vleeschouwer, M. Vahlenkamp, M. Crucifix, H. Pälike, *Geology* **45**, 375–378 (2017).
6. O. Friedrich, R. D. Norris, J. Erbacher, *Geology* **40**, 107–110 (2012).
7. K. G. Miller, R. G. Fairbanks, G. S. Mountain, *Paleoceanography* **2**, 1–19 (1987).
8. J. Veizer, A. Prokoph, *Earth Sci. Rev.* **146**, 92–104 (2015).
9. J. C. Zachos, G. R. Dickens, R. E. Zeebe, *Nature* **451**, 279–283 (2008).
10. K. G. Miller, J. V. Browning, W. J. Schmelz, R. E. Kopp, G. S. Mountain, J. D. Wright, Cenozoic sea-level and cryospheric evolution from deep-sea geochemical and continental margin records. *Sci. Adv.* **6**, eaaz1346 (2020).
11. A. J. Drury, T. Westerhold, D. Hodell, U. Röhl, *Clim. Past* **14**, 321–338 (2018).
12. M. E. Katz, D. R. Katz, J. D. Wright, K. G. Miller, D. K. Pak, N. J. Shackleton, E. Thomas, Early Cenozoic benthic foraminiferal isotopes: Species reliability and interspecies correction factors. *Paleoceanography* **18**, 1024 (2003).
13. See supplementary materials.
14. J. Laskar, A. Fienga, M. Gastineau, H. Manche, *Astron. Astrophys.* **532**, A89 (2011).
15. N. Marwan, M. C. Romano, M. Thiel, J. Kurths, *Phys. Rep.* **438**, 237–329 (2007).
16. T. Westerhold, U. Röhl, B. Donner, J. C. Zachos, *Paleoceanogr. Paleoclimatol.* **33**, 626–642 (2018).
17. H. K. Coxall, P. A. Wilson, H. Pälike, C. H. Lear, J. Backman, *Nature* **433**, 53–57 (2005).
18. J. F. Spray et al., *Paleoceanogr. Paleoclimatol.* **34**, 1124–1138 (2019).
19. B. P. Flower, J. P. Kennett, The middle Miocene climatic transition: East Antarctic ice sheet development, deep ocean circulation and global carbon cycling. *Pal. Pal. Pal.* **108**, 537–555 (1994).
20. A. E. Holbourn, W. Kuhnt, K. G. D. Kochhann, N. Andersen, K. J. Sebastian Meier, *Geology* **43**, 123–126 (2015).
21. D. A. Hodell, K. A. Venz-Curtis, Late Neogene history of deepwater ventilation in the Southern Ocean. *Geochem. Geophys. Geosyst.* **7**, Q09001 (2006).
22. A. J. Drury et al., *Earth Planet. Sci. Lett.* **475**, 254–266 (2017).
23. S. K. Turner, *Paleoceanography* **29**, 1256–1266 (2014).
24. I. Bailey et al., *Quat. Sci. Rev.* **75**, 181–194 (2013).
25. T. Laepple, G. Lohmann, Seasonal cycle as template for climate variability on astronomical timescales. *Paleoceanography* **24**, PA4201 (2009).
26. T. Westerhold, U. Röhl, *Clim. Past* **5**, 309–327 (2009).
27. M. Vahlenkamp et al., *Earth Planet. Sci. Lett.* **484**, 329–340 (2018).
28. T. J. Crowley, K.-Y. Kim, J. G. Mengel, D. A. Short, *Science* **255**, 705–707 (1992).
29. D. A. Short, J. G. Mengel, T. J. Crowley, W. T. Hyde, G. R. North, *Quat. Res.* **35**, 157–173 (1991).
30. R. E. Zeebe, T. Westerhold, K. Littler, J. C. Zachos, *Paleoceanography* **32**, 440–465 (2017).
31. K. E. Trenberth, D. P. Stepaniak, J. M. Caron, *J. Clim.* **13**, 3969–3993 (2000).
32. P. X. Wang et al., *Earth Sci. Rev.* **174**, 84–121 (2017).
33. M. Huber, A. Goldner, *J. Asian Earth Sci.* **44**, 3–23 (2012).
34. J. H. C. Bosmans, S. S. Drijfhout, E. Tuenter, F. J. Hilgen, L. J. Lourens, *Clim. Dyn.* **44**, 279–297 (2015).
35. H. Pälike et al., *Science* **314**, 1894–1898 (2006).
36. A. E. Holbourn, W. Kuhnt, S. Clemens, W. Prell, N. Andersen, *Paleoceanography* **28**, 688–699 (2013).
37. S. R. Meyers, L. A. Hinnov, Northern Hemisphere glaciation and the evolution of Plio-Pleistocene climate noise. *Paleoceanography* **25**, PA3207 (2010).
38. D. Liebrand, A. T. M. de Bakker, *Clim. Past* **15**, 1959–1983 (2019).
39. S. Kirtland Turner, P. F. Sexton, C. D. Charles, R. D. Norris, *Nat. Geosci.* **7**, 748–751 (2014).
40. D. J. Lunt et al., *Nat. Geosci.* **4**, 775–778 (2011).
41. V. Dakos et al., *Proc. Natl. Acad. Sci. U.S.A.* **105**, 14308–14312 (2008).
42. M. Scheffer et al., *Nature* **461**, 53–59 (2009).
43. W. Steffen et al., *Proc. Natl. Acad. Sci. U.S.A.* **115**, 8252–8259 (2018).
44. M. D. Palmer, G. R. Harris, J. M. Gregory, *Environ. Res. Lett.* **13**, 084003 (2018).
45. T. Westerhold, Cenozoic global reference benthic carbon and oxygen isotope dataset (CENOGRID). PANGAEA (2020); https://doi.pangaea.de/10.1594/PANGAEA.917503.

SUPPLEMENTARY MATERIALS

science.sciencemag.org/content/369/6509/1383/suppl/DC1
Materials and Methods
Supplementary Text S1 to S4
Figs. S1 to S35
Tables S1 to S34
References (46–184)

Science

An astronomically dated record of Earth's climate and its predictability over the last 66 million years

Thomas Westerhold, Norbert Marwan, Anna Joy Drury, Diederik Liebrand, Claudia Agnini, Eleni Anagnostou, James S. K. Barnet, Steven M. Bohaty, David De Vleeschouwer, Fabio Florindo, Thomas Frederichs, David A. Hodell, Ann E. Holbourn, Dick Kroon, Vittoria Lauretano, Kate Littler, Lucas J. Lourens, Mitchell Lyle, Heiko Pälike, Ursula Röhl, Jun Tian, Roy H. Wilkens, Paul A. Wilson and James C. Zachos

The states of past climate

Deep-sea benthic foraminifera preserve an essential record of Earth's past climate in their oxygen- and carbon-isotope compositions. However, this record lacks sufficient temporal resolution and/or age control in some places to determine which climate forcing and feedback mechanisms were most important. Westerhold *et al.* present a highly resolved and well-dated record of benthic carbon and oxygen isotopes for the past 66 million years. Their reconstruction and analysis show that Earth's climate can be grouped into discrete states separated by transitions related to changing greenhouse gas levels and the growth of polar ice sheets. Each climate state is paced by orbital cycles but responds to variations in radiative forcing in a state-dependent manner.
Science, this issue p. 1383

ARTICLE TOOLS	http://science.sciencemag.org/content/369/6509/1383
SUPPLEMENTARY MATERIALS	http://science.sciencemag.org/content/suppl/2020/09/09/369.6509.1383.DC1
REFERENCES	This article cites 175 articles, 31 of which you can access for free http://science.sciencemag.org/content/369/6509/1383#BIBL
PERMISSIONS	http://www.sciencemag.org/help/reprints-and-permissions

Use of this article is subject to the Terms of Service